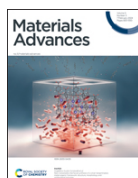




Network access provided by: **University of California - San Diego**





From the journal:

**Materials Advances**

## 3D bioprinting cowpea mosaic virus as an immunotherapy depot for ovarian cancer prevention in a preclinical mouse model †

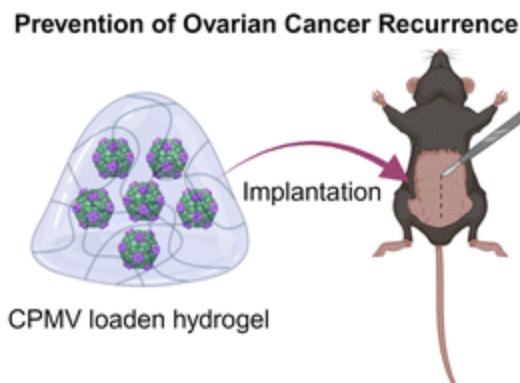


[Zhongchao Zhao](#),  ‡<sup>abc</sup> [Yi Xiang](#), ‡<sup>a</sup> [Edward C. Koellhoffer](#),<sup>d</sup> [Sourabh Shukla](#),<sup>a</sup> [Steven Fiering](#),<sup>ef</sup> [Shaochen Chen](#)<sup>\*abgh</sup> and [Nicole F. Steinmetz](#)  \*<sup>abcdghij</sup>

[Author affiliations](#)

### Abstract

Implantable polymeric hydrogels loaded with immunostimulatory cowpea mosaic virus (CPMV) were fabricated using digital light processing (DLP) printing technology. The CPMV-laden hydrogels were surgically implanted into the peritoneal cavity to serve as depots for cancer slow-release immunotherapy. Sustained release of CPMV within the intraperitoneal space alleviates the need for repeated dosing and we demonstrated efficacy against ovarian cancer in a metastatic mouse model.



Serous ovarian cancer is a deadly malignancy for women, and about 80% of patients are diagnosed at advanced stages with metastatic disease in the peritoneal space.<sup>1-3</sup> Standard care for women with ovarian cancer is surgical debulking followed by platinum-based chemotherapy. Although these treatments can provide a short period of remission, up to 70% of patients experience recurrence.<sup>3,4</sup> Despite the advances of immunotherapy for cancer treatment, there is no established immunotherapy for ovarian cancer. There is a dire need for therapeutic innovation and development of treatment strategies that prolong survival and prevent recurrence. Immunotherapy is an undeveloped therapeutic option for this disease.

Cancer immunotherapy is fundamentally different from and has multiple advantages over cytotoxic chemotherapy. Immunotherapy empowers the patient's own immune system to recognize and eliminate tumors and metastasis and when anti-tumor immune memory is established, treatment responses can be durable preventing recurrence. Using mouse models of aggressive metastatic ovarian cancer, we have previously reported that the plant virus, cowpea mosaic virus (CPMV), is a potent cancer immunotherapy that generates durable anti-tumor immune responses against ovarian cancer. Weekly intraperitoneal (i.p.) dosing of immunomodulatory CPMV nanoparticles effectively reprograms the ovarian tumor microenvironment (TME) within the i.p. space, leading to survival benefit with inhibited tumor growth, extended survival, and protection demonstrated by re-challenge experiments.<sup>5,6</sup> The potent efficacy of CPMV has been established in various solid tumor types including in canine patients with spontaneous tumors.<sup>5-10</sup> Mechanism studies demonstrate that CPMV is a toll-like receptor agonist of TLR2, 4, and 7 and this initially stimulates and recruits immune stimulatory innate immune cells to the tumor sites. Tumor cell killing is mediated by these innate immune cells, which then become antigen-presenting cells to establish adaptive and systemic anti-tumor immunity.<sup>11,12</sup> To achieve this potency and effectively overcome the immunosuppressed TME, repeated i.p. injections are required. However, this bears a translational barrier because i.p. administration in humans is a complex procedure and requires hospitalization that increases cost and decreases quality of life;<sup>13</sup> repeated i.p. dosing will be challenging to implement in any clinical treatment plan. To overcome this technological barrier, we turned toward the formulation of CPMV

hydrogels to form an intraperitoneal depot that mediates sustained release, thus alleviating the need for repeated dosing. Given that women with ovarian cancer almost always require surgeries to remove tumor tissues, such a CPMV hydrogel biomedical device could be readily implanted post-surgical debulking along with CPMV priming. Therefore, no future surgical operation will be needed.

Various slow-release formulations have been developed, such as hydrogels for vaccine or chemotherapy delivery,<sup>14,15</sup> as well as microparticle depots or microneedle patches for immunotherapy/antibody delivery.<sup>16,17</sup> In a previous study we turned toward a CPMV-dendrimer self-assembly strategy to form i.p. CPMV depots and showed that the CPMV-dendrimer co-assemblies served as slow-release CPMV formulation and achieved improved efficacy against ovarian cancer after a single treatment.<sup>18</sup> While efficacious in the tumor mouse model, translation may be hampered due to toxicity of the dendrimer formulations;<sup>19,20</sup> another hurdle is that the formulation relied on self-assembly primed by electrostatic interactions leading to nanoscale aggregates with ill-defined size control.

3D bioprinting is an additive manufacturing strategy for the fabrication of bio-constructs. To date, extrusion-, inkjet-, and light- based 3D bioprinting strategies have been developed to print constructs with live cells, biomaterials, or biological molecules, which constitute bioinks. Extrusion-based and inkjet-based bioprinting feature the precise deposition of the bioink with defined placement and pattern.<sup>21,22</sup> Light-based printing, featuring digital light processing (DLP) printing, uses light to selectively initiate bioink photopolymerization in a vat, enabling layer-by-layer construction with fine control over the geometry of the structure.<sup>23</sup> Compared to extrusion- and inkjet-based bioprinting, DLP printing exhibits significant advantages in printing speed, making it promising for large-scale manufacturing.<sup>24</sup> DLP printing is also less dependent than extrusion printing or inkjet printing on specific rheological properties of the bioinks.<sup>21,22</sup> Additionally, DLP printing offers excellent printing resolution, achieving details up to micron-scale.<sup>25</sup> Overall, the DLP bioprinting technology will not only enable us to formulate biodegradable and biosafe 3D depot but also offer us more engineering space to incorporate various antigens and adjuvants in our future cancer immunotherapy development.

In this work we sought to explore the feasibility of using DLP<sup>26,27</sup> printing technology to fabricate biocompatible polymeric CPMV-laden hydrogels of defined size and geometry ([Fig. 1A](#)), to establish this platform for future development of more complex systems. First, CPMV was propagated in black eyed peas and purified as previously described.<sup>28,29</sup> Then, CPMV was mixed with a defined concentration of gelatin methacrylate (GelMA, 4% w/v) and Polyethylene glycol diacrylate (PEGDA, 0.1% w/v) to prepare a bioink, which was then exposed to 405 nm light for 30 s (light intensity = 79.4 mW cm<sup>-2</sup>) to achieve polymerization and hydrogel formation. Hydrogels of 9.5 mm × 6 mm × 3.2 mm in a slab geometry were bioprinted containing 900 µg CPMV. The polymerization process and blending of CPMV were characterized by Fourier-transform infrared spectroscopy (FTIR). Acrylate polymerization was effectively initiated for both CPMV laden-hydrogel and sham hydrogel with no CPMV during the DLP printing process, as validated by the

pronounced drop in transmittance at  $1640\text{ cm}^{-1}$  (Fig. 1B). Upon the incorporation of CPMV, a group of subtle absorbance signals were noted around  $\sim 3000\text{ cm}^{-1}$ . However, the spectrum did not display any characteristic absorbance indicative of covalent or non-covalent bonding. This suggests that CPMV was incorporated into the hydrogel through simple blending, which led to a diffusion-based release mechanism. The microarchitecture was examined by scanning electron microscopic (SEM) imaging of the lyophilized samples. A porous hydrogel architecture stemming from, and characteristic for, the polymeric network of GelMA and PEGDA was observed (Fig. 1C). A consistent pore size distribution was observed in both samples; data suggest that CPMV did not disrupt the polymerization. Mechanical testing further corroborated this, as sham and CPMV-laden hydrogels exhibited comparable Young's moduli (Sham gel:  $6531 \pm 628.0\text{ Pa}$ , CPMV gel:  $6117 \pm 2670\text{ Pa}$ ,  $p = 0.8065$ ) (Fig. 1D). *In vitro* release of the bioprinted CPMV in PBS was evaluated by ELISA.<sup>26</sup>  $\sim 30\%$  of CPMV was released by day 1, and  $\sim 50\%$  of CPMV was released by day 3. The release then continued slowly to day 14 when it reached a plateau of  $\sim 60\%$ , which followed the pattern of Fick's diffusion<sup>30</sup> (Fig. 1E).



**Fig. 1** Bioprinting and characterization of CPMV implants. (A) Schematic diagram of the digital light processing (DLP) bioprinting approach. Characterization of empty gel (Sham) and CPMV loaded implants using (B) FTIR spectroscopy, (C) SEM, and (D) Young's modulus (statistical analysis was calculated by unpaired T test) (D). (E) *In vitro* releasing profile of printed CPMV.

To evaluate the sustained release of CPMV within the i.p. space, we generated hydrogels incorporating Cy5-labeled CPMV (CPMV-Cy5). Each CPMV particle offers 300 surface-exposed lysine residues suitable for bioconjugation using N-hydroxysuccinimide (NHS) chemistry.<sup>31</sup> To synthesize CPMV-Cy5, CPMV was reacted with sulfo-Cy5-NHS ester using previously established protocol.<sup>29,32</sup> As demonstrated by the denaturing gel electrophoresis (NuPAGE), Cy5 signal co-migrated with the CPMV coat proteins, demonstrating the successful conjugation of Cy5 to CPMV (Fig. S1A, ESI †). UV-Vis spectrophotometry analysis determined that  $\sim 78$  Cy5 molecules were conjugated per CPMV (Fig. S1A, ESI †). Transmission electron microscopy confirmed that CPMV-Cy5 remained intact and structural sound similar to unconjugated CPMV (Fig. S1C, ESI †). Subsequently, we loaded  $600\text{ }\mu\text{g}$  of CPMV-Cy5 into two distinct hydrogel formulations: one comprising 5% GelMA + 0.2% PEGDA and the other containing 4% GelMA + 0.1% PEGDA. This allowed us to investigate whether the *in vivo* release of CPMV could be modulated by the formulation;  $600\text{ }\mu\text{g}$  soluble CPMV-Cy5 was i.p. injected as a control. To validate that the CPMV-laden hydrogels formed a depot for sustained CPMV release *in vivo*, CPMV-Cy5-loaded hydrogels were surgically implanted into the i.p. space of BALB/c mice, and Cy5 fluorescence was continuously monitored and

recorded for a duration of 30 days. The two formulations are designed to provide different kinetics of release – a higher GelMA and PEGDA concentration created a denser polymeric network to sustain the diffusion of CPMV and lead to a slower release.<sup>33</sup> PEGDA increases the stiffness of the implant and therefore improves its handleability. The formulation with 0.1% PEGDA is softer and therefore more compatible to the mechanical environment of the peritoneal although it required more skillful handling for the implantation. Upon surgical administration of the CPMV-laden hydrogels and i.p. injection of CPMV-Cy5, the Cy5 fluorescence signal within the i.p. space was monitored by IVIS imaging ([Fig. 2A](#)). Quantitative analysis showed an initial decrease followed by a gradual increase in fluorescence intensity for both hydrogel formulations – this fluctuation can be explained by initial fluorescence quenching.<sup>34</sup> At day 15 post administration, maximum fluorescence intensity was achieved for both hydrogels, then the fluorescence signals declined gradually for 30 days post administration, which indicated the sustained release of CPMV in the i.p. space ([Fig. 2B](#)). In comparison, the soluble CPMV-Cy5 showed early increasing of Cy5 fluorescence with peaking around day 7 and faster decay over time. Overall, no major differences in the release profiles were noted comparing the two hydrogel formulations; therefore, we proceeded with 4% GelMA + 0.1% PEGDA for efficacy testing.



**Fig. 2** Release of CPMV in the intraperitoneal space. (A) Fluorescence imaging of BALB/c mice post-surgical implantation of CPMV-Cy5 hydrogels on days 0, 14, and 27. (B) Quantified fluorescent intensity in the intraperitoneal space over time.

Next, we assessed the efficacy of the CPMV slow-release hydrogel using a mouse model of ovarian cancer, ID8-Defb29/Vegf-a-Luc ovarian tumors, disseminated in the peritoneal cavity of C57BL/6J mice.<sup>35,36</sup> To mimic the remission stage and application of the implant post-surgery, we first surgically implanted hydrogels containing 900  $\mu\text{g}$  of CPMV into the i.p. space on day  $-3$  prior to tumor challenge. In addition, we administered a single dose of soluble CPMV (100  $\mu\text{g}$  in 200  $\mu\text{L}$  of PBS, i.p.). The addition of soluble CPMV is to kick-start the immunostimulation and avoid delayed responses due to slow-release of CPMV from the hydrogel ( $n = 9$ ). The slow-release hydrogel group was compared to: (1) soluble 1 mg dose of CPMV (i.p. administration,  $n = 9$ ), (2) weekly administration of 100  $\mu\text{g}$ -doses of CPMV (in 200  $\mu\text{L}$  of PBS, weekly for 6 weeks,  $n = 10$ ). PBS ( $n = 8$ ) and sham gel ( $n = 9$ ) were included as controls ([Fig. 3A](#)). On day 0, mice were challenged with  $5 \times 10^6$  ID8-Defb29/Vegf-a-Luc cells administered i.p. Tumor progression was monitored closely by tracking changes in body weight ([Fig. S2A and B](#), ESI †) and increases in body circumference ([Fig. 3B and C](#)) due to tumor burden and ascites. On day 50, all groups received one additional dose of 100  $\mu\text{g}$  soluble CPMV *via* i.p. injection to further improve treatment efficacy. The study concluded on day 80

when all remaining mice were free of tumors. Mice were euthanized if ascites and tumor growth caused body weight to exceed 35 g or their abdominal circumference exceeded 9 cm.<sup>6</sup>



**Fig. 3** Treatment efficacy of CPMV hydrogels. (A) Treatment and tumor injection schedule. The groups are PBS ( $n=8$ ), Sham hydrogel ( $n=9$ ), CPMV hydrogel (900  $\mu\text{g}$  + 100  $\mu\text{g}$  soluble CPMV) ( $n=9$ ), bolus treatment (1 mg CPMV) ( $n=9$ ), and weekly CPMV dosing using 100  $\mu\text{g}$  ( $n=10$ ). (B) Individual circumferences in each group. (C) Average body circumferences for all treatment groups. Data points are cut off when  $n < 5$  for the treatment group. (D) Survival rates for all treatment groups. Statistical significance in (C) was calculated by two-way ANOVA (\*\* $p < 0.01$ , \*\*\* $p < 0.001$ , \*\*\*\* $p < 0.0001$ ). Statistical significance in (D) was calculated using the log-rank (Mantel–Cox) test (\*\* $p < 0.01$ , \*\*\*\* $p < 0.0001$ ).

The weekly dosing of 100  $\mu\text{g}$  CPMV is the established ‘standard dose’ for the ID8-Defb29/Vegf-a-Luc i.p. ovarian cancer model in C57BL/6J mice,<sup>5,7</sup> consistent with our prior work.<sup>5–7</sup> This repeated dosing of CPMV indeed showed potent efficacy controlling tumor growth and leading to survival benefits ([Fig. 3B–D](#)). Also, the surgically implanted CPMV hydrogels primed potent efficacy against the ovarian tumors and appeared slightly more potent in terms of controlling tumor growth and survival rate ([Fig. 3B–D](#)). Lastly, the 1 mg bolus-dose of CPMV also delayed onset of tumor growth, however with lesser efficacy compared to the sustained-release or repeated dosing groups. This underscores the potent anti-tumor efficacy of CPMV. Conversely, the sham hydrogel group or PBS control groups had no discernible effects on tumor growth. While statistical significance was not reached, sustained release CPMV hydrogel treatment trended toward being the most potent formulation as demonstrated by improved controlling of tumor growth ([Fig. 3B and C](#)) and enhanced overall survival rates (33.3%, 3/9 mice) in comparison to repetitive dosing (30%, 3/10) and bolus dosing (22.2%, 2/9) ([Fig. 3D](#)). Further analysis revealed that CPMV gel implantation extended median survival to 66 days, compared to 60 days with repetitive CPMV dosing and 52 days with a single large CPMV dose. In contrast, both PBS and Sham gel controls had a median survival of 44 days. It was noted that the single bolus CPMV dose of 1 mg, resulted in five mice displaying potential autoimmune symptoms, such as fur loss and white hair growth. From a clinical perspective, CPMV hydrogel implants not only prevent overdosing and excessive immune system overstimulation but also ensure efficacy with a broader remission period for patients to receive additional treatments. This approach can also reduce costs associated with repetitive dosing and hospitalization, ultimately leading to an improved quality of life.

In conclusion, we successfully developed a sustained-release hydrogel formulation of CPMV using state-of-the-art DLP printing technology. Sustained release of the active ingredient, CPMV, was confirmed through *in vitro* and longitudinal imaging studies in live animals. More importantly, through surgical

implantation, the CPMV-laden hydrogels proved potent and efficacious against murine ovarian cancer – on par with our standard weekly dosing regimen. From a clinical perspective, CPMV hydrogel implantation offers several advantages over the traditional dosing methods by avoiding repetitive intraperitoneal injection with associated patient stress, potential for problems and increased costs with hospitalization. Less need for repetitive clinical intervention will enhance quality of life for patients, and the slow release potentially would reduce risk of immune-related adverse events. Throughout this study, the hydrogels served as scaffolds for CPMV delivery. In our forthcoming research, we aim to enhance treatment efficacy for ovarian cancer by incorporating additional immunoadjuvants or tumor-specific antigens. Overall, this work lays the groundwork for the future translation of CPMV as a treatment option for human patients in clinical settings.

## Author contributions

Z. Z., Y. X., S. F., S. C., and N. F. S. designed and analyzed experiments. Z. Z., Y. X., E. C. K., and S. S. performed experiments. Z. Z., Y. X., S. C., and N. F. S. wrote the manuscript. Z. Z. and Y. X., contributed equally.

## Conflicts of interest

The authors declare the following competing financial interest(s): Dr Steinmetz and Dr Fiering are co-founders and have equity and financial interest in Mosaic ImmunoEngineering Inc. Dr Steinmetz is a co-founder of, and serves as manager of Pokometz Scientific LLC, under which she is a paid consultant to Mosaic ImmunoEngineering Inc., Flagship Labs 95 Inc., and Arana Biosciences Inc. The other authors declare no potential COI.

## Acknowledgements

This work was supported in part by the NIH (R01-CA253615) to N. F. S., S. C. and S. F., the Shaughnessy Family Fund for Nano-ImmunoEngineering (nanoIE) at the University of California, San Deigo (UCSD), and training grant T32EB005970 to E. C. K. We thank the Nano3 core facility at UCSD for transmission electron microscopy imaging. Nano3 hosts San Diego Nanotechnology Infrastructure (SDNI), a member of the National Nanotechnology Coordinated Infrastructure (NNCI), which is supported by the National Science Foundation (Grant ECCS-2025752).

## References



1. P. A. T. E. Board, Ovarian Epithelial, Fallopian Tube, and Primary Peritoneal Cancer Treatment (PDQ®), In PDQ Cancer Information Summaries [Internet], National Cancer Institute (US), 2021.
2. T. Arora , S. Mullangi and M. R. Lekkala , *Ovarian cancer* , StatPearls [Internet], 2022, [Search PubMed](#)  .
3. R. L. Siegel , K. D. Miller , H. E. Fuchs and A. Jemal , Cancer Statistics, 2021, *Ca-Cancer J. Clin.*, 2021, **71** , 7 —33 [CrossRef](#) [PubMed](#)  .
4. C. Della Pepa , G. Tonini , C. Pisano , M. Di Napoli , S. C. Cecere , R. Tambaro , G. Facchini and S. Pignata , Ovarian cancer standard of care: are there real alternatives?, *Chin. J. Cancer*, 2015, **34** , 17 —27 [CrossRef](#) [CAS](#) [PubMed](#)  .
5. C. Wang , S. N. Fiering and N. F. Steinmetz , Cowpea Mosaic Virus Promotes Anti-Tumor Activity and Immune Memory in a Mouse Ovarian Tumor Model, *Adv. Ther.*, 2019, **2** , 5 [Search PubMed](#)  .
6. S. Shukla , C. Wang , V. Beiss , H. Cai , T. Washington 2nd , A. A. Murray , X. Gong , Z. Zhao , H. Masarapu , A. Zlotnick , S. Fiering and N. F. Steinmetz , The unique potency of Cowpea mosaic virus (CPMV) in situ cancer vaccine, *Biomater. Sci.*, 2020, **8** , 5489 —5503 [RSC](#)  .
7. P. H. Lizotte , A. M. Wen , M. R. Sheen , J. Fields , P. Rojasopondist , N. F. Steinmetz and S. Fiering , In situ vaccination with cowpea mosaic virus nanoparticles suppresses metastatic cancer, *Nat. Nanotechnol.*, 2016, **11** , 295 —303 [CrossRef](#) [CAS](#) [PubMed](#)  .
8. P. J. Hoopes , R. J. Wagner , K. Duval , K. Kang , D. J. Gladstone , K. L. Moodie , M. Crary-Burney , H. Ariaspulido , F. A. Veliz , N. F. Steinmetz and S. N. Fiering , Treatment of Canine Oral Melanoma with Nanotechnology-Based Immunotherapy and Radiation, *Mol. Pharmaceutics*, 2018, **15** , 3717 —3722 [CrossRef](#) [CAS](#) [PubMed](#)  .
9. D. Alonso-Miguel , G. Valdivia , D. Guerrero , M. D. Perez-Alenza , S. Pantelyushin , A. Alonso-Diez , V. Beiss , S. Fiering , N. F. Steinmetz and M. Suarez-Redondo , Neoadjuvant in situ vaccination with cowpea mosaic virus as a novel therapy against canine inflammatory mammary cancer, *J. Immunother. Cancer.*, 2022, **10** , 3 [Search PubMed](#)  .
10. Y. H. Chung , J. Park , H. Cai and N. F. Steinmetz , S100A9-Targeted Cowpea Mosaic Virus as a Prophylactic and Therapeutic Immunotherapy against Metastatic Breast Cancer and Melanoma, *Adv. Sci.*, 2021, **8** , 2101796 [CrossRef](#) [CAS](#) [PubMed](#)  .
11. C. Mao , V. Beiss , J. Fields , N. F. Steinmetz and S. Fiering , Cowpea mosaic virus stimulates antitumor immunity through recognition by multiple MYD88-dependent toll-like receptors, *Biomaterials*, 2021, **275** , 120914 [CrossRef](#) [CAS](#) [PubMed](#)  .
12. C. Wang , V. Beiss and N. F. Steinmetz , Cowpea Mosaic Virus Nanoparticles and Empty Virus-Like Particles Show Distinct but Overlapping Immunostimulatory Properties, *J. Virol.*, 2019, **93** , 21 [Search PubMed](#)  .




13. A. A. Wright , A. Cronin , D. E. Milne , M. A. Bookman , R. A. Burger , D. E. Cohn , M. C. Cristea , J. J. Griggs , N. L. Keating and C. F. Levenback , Use and effectiveness of intraperitoneal chemotherapy for treatment of ovarian cancer, *Obstet. Gynecol. Surv.*, 2015, **70** , 696 —697 [CrossRef](#)  .
14. Y. Umeki , K. Mohri , Y. Kawasaki , H. Watanabe , R. Takahashi , Y. Takahashi , Y. Takakura and M. Nishikawa , Induction of potent antitumor immunity by sustained release of cationic antigen from a DNA-based hydrogel with adjuvant activity, *Adv. Funct. Mater.*, 2015, **25** , 5758 —5767 [CrossRef](#) [CAS](#)  .
15. K. Yamaguchi , O. Hiraike , H. Iwaki , K. Matsumiya , N. Nakamura , K. Sone , S. Ohta , Y. Osuga and T. Ito , Intraperitoneal administration of a cisplatin-loaded nanogel through a hybrid system containing an alginic acid-based nanogel and an in situ cross-linkable hydrogel for peritoneal dissemination of ovarian cancer, *Mol. Pharmaceutics*, 2021, **18** , 4090 —4098 [CrossRef](#) [CAS](#) [PubMed](#)  .
16. M. F. Fransen , R. A. Cordfunke , M. Sluijter , M. J. Van Steenberghe , J. W. Drijfhout , F. Ossendorp , W. E. Hennink and C. J. Melief , Effectiveness of slow-release systems in CD40 agonistic antibody immunotherapy of cancer, *Vaccine*, 2014, **32** , 1654 —1660 [CrossRef](#) [CAS](#) [PubMed](#)  .
17. C. Wang , Y. Ye , G. M. Hochu , H. Sadeghifar and Z. Gu , Enhanced cancer immunotherapy by microneedle patch-assisted delivery of anti-PD1 antibody, *Nano Lett.*, 2016, **16** , 2334 —2340 [CrossRef](#) [CAS](#) [PubMed](#)  .
18. A. E. Czapar , B. D. B. Tiu , F. A. Veliz , J. K. Pokorski and N. F. Steinmetz , Slow-release formulation of cowpea mosaic virus for in situ vaccine delivery to treat ovarian cancer, *Adv. Sci.*, 2018, **5** , 1700991 [CrossRef](#) [PubMed](#)  .
19. S. P. Mukherjee , F. M. Lyng , A. Garcia , M. Davoren and H. J. Byrne , Mechanistic studies of in vitro cytotoxicity of poly (amidoamine) dendrimers in mammalian cells, *Toxicol. Appl. Pharmacol.*, 2010, **248** , 259 —268 [CrossRef](#) [CAS](#) [PubMed](#)  .
20. L. Albertazzi , L. Gherardini , M. Brondi , S. Sulis Sato , A. Bifone , T. Pizzorusso , G. M. Ratto and G. Bardi , In vivo distribution and toxicity of PAMAM dendrimers in the central nervous system depend on their surface chemistry, *Mol. Pharmaceutics*, 2013, **10** , 249 —260 [CrossRef](#) [CAS](#) [PubMed](#)  .
21. W. L. Ng , X. Huang , V. Shkolnikov , R. Suntornnond and W. Y. Yeong , Polyvinylpyrrolidone-based bioink: influence of bioink properties on printing performance and cell proliferation during inkjet-based bioprinting, *Bio-Des. Manuf.*, 2023, **6** , 676 —690 [CrossRef](#) [CAS](#)  .
22. Y. S. Zhang , G. Haghashtiani , T. Hübscher , D. J. Kelly , J. M. Lee , M. Lutolf , M. C. McAlpine , W. Y. Yeong , M. Zenobi-Wong and J. Malda , 3D extrusion bioprinting, *Nat. Rev. Methods Primers*, 2021, **1** , 75 [CrossRef](#) [CAS](#)  .
23. R. Levato , O. Dudaryeva , C. E. Garciamendez-Mijares , B. E. Kirkpatrick , R. Rizzo , J. Schimelman , K. S. Anseth , S. Chen , M. Zenobi-Wong and Y. S. Zhang , Light-based vat-polymerization bioprinting, *Nat. Rev. Methods Primers*, 2023, **3** , 47 [CrossRef](#) [CAS](#)  .

24. J. Wu , J. Guo , C. Linghu , Y. Lu , J. Song , T. Xie and Q. Zhao , Rapid digital light 3D printing enabled by a soft and deformable hydrogel separation interface, *Nat. Commun.*, 2021, **12** , 6070 [CrossRef](#) [CAS](#) [PubMed](#)  .
25. J. L. Sanchez Noriega , N. A. Chartrand , J. C. Valdoz , C. G. Cribbs , D. A. Jacobs , D. Poulson , M. S. Viglione , A. T. Woolley , P. M. Van Ry and K. A. Christensen , Spatially and optically tailored 3D printing for highly miniaturized and integrated microfluidics, *Nat. Commun.*, 2021, **12** , 5509 [CrossRef](#) [CAS](#) [PubMed](#)  .
26. J. F. Affonso de Oliveira , Z. Zhao , Y. Xiang , M. D. Shin , K. E. Villaseñor , X. Deng , S. Shukla , S. Chen and N. F. Steinmetz , COVID-19 vaccines based on viral nanoparticles displaying a conserved B-cell epitope show potent immunogenicity and a long-lasting antibody response, *Front. Microbiol.*, 2023, **14** , 1117494 [CrossRef](#) [PubMed](#)  .
27. J. Liu , K. Miller , X. Ma , S. Dewan , N. Lawrence , G. Whang , P. Chung , A. D. McCulloch and S. Chen , Direct 3D bioprinting of cardiac micro-tissues mimicking native myocardium, *Biomaterials*, 2020, **256** , 120204 [CrossRef](#) [CAS](#) [PubMed](#)  .
28. A. M. Wen , K. L. Lee , I. Yildiz , M. A. Bruckman , S. Shukla and N. F. Steinmetz , Viral nanoparticles for in vivo tumor imaging, *J. Visualized Exp.*, 2012, **69** , e4352 [Search PubMed](#)  .
29. Z. Zhao , O. A. Ortega-Rivera , Y. H. Chung , A. Simms and N. F. Steinmetz , A co-formulated vaccine of irradiated cancer cells and cowpea mosaic virus improves ovarian cancer rejection, *J. Mater. Chem. B*, 2023, **11** , 5429 —5441 [RSC](#)  .
30. G. Guevara-Carrion , R. Fingerhut and J. Vrabec , Fick diffusion coefficient matrix of a quaternary liquid mixture by molecular dynamics, *J. Phys. Chem. B*, 2020, **124** , 4527 —4535 [CrossRef](#) [CAS](#) [PubMed](#)  .
31. A. Chatterji , W. F. Ochoa , M. Paine , B. R. Ratna , J. E. Johnson and T. Lin , New addresses on an addressable virus nanoblock; uniquely reactive Lys residues on cowpea mosaic virus, *Chem. Biol.*, 2004, **11** , 855 —863 [CrossRef](#) [CAS](#) [PubMed](#)  .
32. Y. H. Chung , H. Cai and N. F. Steinmetz , Viral nanoparticles for drug delivery, imaging, immunotherapy, and theranostic applications, *Adv. Drug Delivery Rev.*, 2020, **156** , 214 —235 [CrossRef](#) [CAS](#) [PubMed](#)  .
33. Y. Xiang , Z. Zhong , E. J. Yao , W. Kiratitanaporn , M. T. Suy and S. Chen , 3D bioprinting of gene delivery scaffolds with controlled release, *Bioprinting*, 2023, **31** , e00270 [CrossRef](#)  .
34. A. M. Wen , M. Infusino , A. De Luca , D. L. Kernan , A. E. Czapar , G. Strangi and N. F. Steinmetz , Interface of physics and biology: engineering virus-based nanoparticles for biophotonics, *Bioconjugate Chem.*, 2015, **26** , 51 —62 [CrossRef](#) [CAS](#) [PubMed](#)  .
35. J. R. Conejo-García , F. Benencia , M.-C. Courreges , E. Kang , A. Mohamed-Hadley , R. J. Buckanovich , D. O. Holtz , A. Jenkins , H. Na and L. Zhang , Tumor-infiltrating dendritic cell precursors recruited by a  $\beta$ -

defensin contribute to vasculogenesis under the influence of Vegf-A, *Nat. Med.*, 2004, **10**, 950—958

[CrossRef](#) [CAS](#) [PubMed](#)  .

36. J. D. Wallat , A. E. Czapar , C. Wang , A. M. Wen , K. S. Wek , X. Yu , N. F. Steinmetz and J. K. Pokorski ,  
Optical and magnetic resonance imaging using fluororous colloidal nanoparticles, *Biomacromolecules*,  
2017, **18** , 103—112 [CrossRef](#) [CAS](#) [PubMed](#)  .

## Footnotes

† Electronic supplementary information (ESI) available: Materials and methods, characterization of CPMV and CPMV-Cy5, recorded mice body weight in the first efficacy study, and averaged circumference and survival rate for the second study.

See DOI: <https://doi.org/10.1039/d3ma00899a>

‡ These authors contributed equally

---

**This journal is © The Royal Society of Chemistry 2024**

About

Cited by

Related

### Download this article

PDF format

Article HTML

## Supplementary files

[Supplementary information](#)

PDF (815K)

## Article information

<https://doi.org/10.1039/D3MA00899A>

**Article type**

Communication

**Submitted**

24 Oct 2023

**Accepted**

22 Jan 2024

**First published**

01 Feb 2024

**This article is Open Access****Citation***Mater. Adv.*, 2024, Advance Article

Go

**Permissions**[Request permissions](#)**Social activity**

Tweet

Share

**Search articles by author**

- Zhongchao Zhao
- Yi Xiang
- Edward C. Koellhoffer
- Sourabh Shukla
- Steven Fiering
- Shaochen Chen

**Nicole F. Steinmetz**

Go

Spotlight

Advertisements



---

> **Journals, books & databases**

---



- Home
- About us
- Membership & professional community
- Campaigning & outreach
- Journals, books & databases
- Teaching & learning
- News & events
- Locations & contacts
- Careers
- Awards & funding
- Advertise
- Help & legal
- Privacy policy
- Terms & conditions



© Royal Society of Chemistry 2024

Registered charity number: 207890